

Wireless Frequency Data Manipulation for Embedded Databases Used in Cybersecurity Applications

Page Heller

Endpoint Security Inc

College Station, TX, USA

email: heller@endpointsecurityinc.com

Abstract— A unique fingerprint in radio frequency signals provides a natural authentication for wireless edge devices in a cybersecurity application based on frequency analysis. Such fingerprints can be improved if extraneous frequency data is removed from the Fourier Transform prior to authentication, but the data manipulation must be done in real time systems with embedded databases designed to store such fingerprints. These embedded systems require a simple and fast process. A method is proposed to manipulate frequency-domain data captured from wireless signals for use in cybersecurity applications to remove unwanted features and ensure the retention of important attributes in embedded databases. Experimental measurements and field studies are presented which lead to modifications in the methodology to address unexpected features encountered. Computational efficiency is taken into account.

Keywords—physical layer cybersecurity; wireless security; Fast Fourier Transform; radio frequency waveforms.

I. INTRODUCTION

Under consideration in this paper is a cybersecurity application which relies on analysis of the frequency content of wireless signals sent from sensors, cameras and actuators that make up what is colloquially referred to as the Internet of Things. This particular application is based on authenticating fixed wireless devices by recognizing a fingerprint in wireless signals unique to each device. The fingerprint is based, in part, on polarization mode dispersion resulting from reflections in a multipath environment [1]. This was previously considered an undesirable trait of wireless communications has become a boon to secure identification of individual transmitting devices [2]. Such dispersion is found to be stable for fixed edge devices and relatively impervious to interference and motion within the multipath. The process may be deployed in applications which use channel-hopping, as well, indicating a broad application area [3][4].

Improvements in the fingerprint may be obtained by removing frequency data that is not specific to the calculation of polarization mode dispersion, specifically, data that is outside the bandwidth of the transmitting device. This often includes side lobe data and data near zero resulting from a transformation from the time domain to frequency domain. Because this authentication must be made as received signals are being demodulated in an access point,

time is of the essence to minimize latency in the data transmission. Therefore, a method is suggested to trim frequency data for such applications in a manner suitable for real time systems employing embedded databases for retaining such fingerprint data. The method is simple and efficient.

To properly address the subject matter of this paper, the following sections are offered. Section II covers background in the area of common implementations of side lobe reduction for applications that are not necessarily real time and embedded systems, so it is possible to envision how the suggested method compares. Section III discusses the theory behind the suggested method for context on why certain decisions were made. Section IV describes the precise signal processing that takes place in the method in a step-by-step manner. Section V shows results of laboratory measurements and modifications made to the method as a result. Section VI shows data from field measurements and further modifications made to the method taking these tests into account. Section VII draws conclusions from observations made in the previous sections.

II. BACKGROUND

Obtaining Radio Frequency (RF) data for the proposed fingerprinting analysis requires receiving a wireless signal, digitizing it and transforming it to the frequency domain. Here, a Discrete Fourier Transform (DFT) is being used for the transformation.

Inherent to the digitization are certain artificial artifacts of the transformation process that may affect future calculations. Primarily targeted in this paper are side lobes in the frequency response data. To remove these, many methods have been proposed for use in applications of radar, radio and ultrasound, dating back to pivotal publications in the 1960s, like Blackman's Data Smoothing and Prediction [5]. The most common of these methods are addressed here.

A. Windowing

Windowing covers a broad area of research in RF waveform manipulation. In this process, a function described mathematically within a fixed window and is multiplied with the signal of interest while being incrementally moved, sample by sample, from one end of the signal to the other, that is, in a sliding window. More precisely, the two functions representing the signal and the window, respectively, are convolved; that is, the integral is taken of

the multiplication of the two functions as in the definition of convolution given in equation (1), where f is the signal function and g is the window function which advances relative to f by frequency bin steps, τ . In this case t refers, not to time, but instead to frequency.

$$(f * g)(t) := \int f(\tau)g(t-\tau) \delta\tau \quad (1)$$

Window functions may be as simple as having a rectangular shape or as complex as a Parzen, Welch, or sine wave. One of the most common is a parabolic shape with three different versions introduced each by Hann, Hamming and Blackman [6][5]. Each has a slightly different effect on modifying the transform, particularly in the area of interest: the side lobes.

Even a simple triangular function can greatly reduce the amplitude of side lobes in RF waveforms. Applications engineers in industry have done extensive studies comparing such techniques in both the time and frequency domains [7]. These methods prove useful in operations that are not time critical and have been found appropriate for displaying the results, for instance. It is even conceivable to use such functions to precondition the waveform in the application under consideration. However, the side lobe data is still present after these convolutions and still troublesome for securely identifying RF fingerprints.

B. Discrete Wavelet Transform

A wireless signal of interest in the application of wireless cybersecurity often travels from transmitter to receiver in an industrial, commercial or residential setting. In these environments, the signal reflects off of many walls, ceilings, floors and objects on its way to the receiver. Such rich multipath channels have caused researchers to investigate other means of transforming received signals into frequency domain data. It is desired to find a transform that is perhaps less sensitive to the distortion and dispersion caused by the multipath. One such method is the Discrete Wavelet Transform, which has been shown to improve the Bit Error Rate (BER) over receivers using the DFT [8][9]. In the case under consideration, however, the dispersion caused by the multipath is of particular interest. There is, therefore, a need to preserve it across the main lobe of the resulting DFT.

C. Subcarrier Weighting

Commonly used in the popular Orthogonal Frequency Division Multiplexing (OFDM) protocols is a concept of subcarrier weighting [10]. In this process of transmitting a wireless signal, each OFDM subcarrier is weighted, that is, multiplied by a fixed or dynamic value used to reduce its impact on adjacent channels. This is commonly done using complex numbers to account for polarization of the signal.

Another similar method has been proposed, which takes computational time into consideration to produce a real time method called advanced subcarrier weighting [11]. Designed primarily for the transmission of signals rather than receiving them, the method reduces side lobe interference with signals in adjacent frequency channels. However, since it is designed

for the transmission side of the data communications, it is not directly applicable to this application.

D. Ultrasound beam summation

Some of the more exotic concepts of dealing with side lobes have come from the medical industry. These application areas are typically centered upon medical imaging, where the frequency domain data is useful in detecting abnormalities or enhancing features of biological images. Methods of beamforming, again on the transmission side, have provided a rich research area for new methods and improvements. One interesting method, which could have mathematical equivalency in received signals, is interference cancellation. For instance, ultrasound beam summation employs pseudo-inverse foci with a second focus located a distance from the initial focus such that the constructive interference between the two signals cancels the side lobes [12]. Although such methods are complex and again centered on transmission, they may lead to interesting developments in received signal manipulation in the future.

E. Other Fingerprinting Methods

Many research approaches to wireless cybersecurity have centered on fingerprinting source devices as a form of authentication. Convolutional Neural Networks (CNNs) have been proposed to fingerprint radios though deep learning of certain inherent hardware features and responses [13][14]. Ongoing research has indicated, however, that wireless multipath channels introduce distortion that negatively affects the reliability of such methods [15].

The new method of cybersecurity authentication with fingerprinting, which is the method under consideration in this paper, employs such distortion for fingerprinting rather than trying to eliminate it. This new method, however, is impacted somewhat negatively by side lobes, which are formed due to the discrete nature of the transformation into the frequency domain. A new approach is sought to remove the undesired features while not creating a burden on real time system computation time.

III. THEORY

In real time embedded system design for radio frequency applications, the primary criterion of concern is execution time. The time required to prepare and store data is a cost subtracted from the total time available to make decisions on actions that must be taken. Thus, the more exotic solutions, although they may produce better results, must give way to the simplest to allow time for the more critical decision-making algorithm.

In the case considered in this paper, execution time is constrained by the requirement to make a decision on the authentication of a received signal prior to the receipt of the next viable signal. A DFT transforms the signal to the frequency domain and further analysis of the dispersion leads to a correlation of the received signal with a known signal. As an example of available time to do this function, using WiFi 802.11n signals transmitted as beacons to search for other devices yields a duration for a signal of around 300 microseconds.

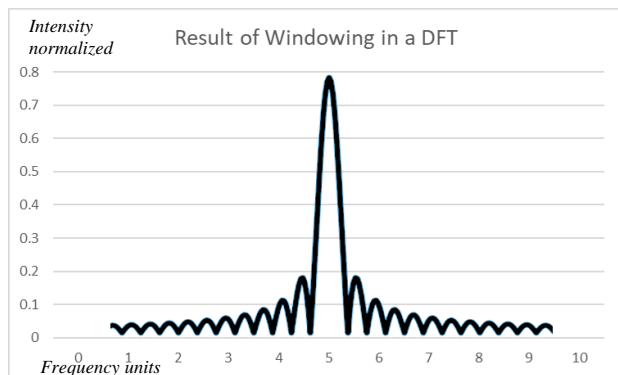


Fig. 1. Windowing data produces side lobes in the results of a DFT on sinusoidal data

By restricting the execution time for data preparation and storage, more time is available for proper authentication. Thus, it is desired to find a way to eliminate unwanted data from the frequency domain data in a short amount of time.

The shape of an ideal DFT resulting from a strong signal, for example one with a Signal-to-Noise Ratio (SNR) of 40 dB, consists of a main lobe centered on the transmitted frequency and side lobes to each side with incrementally lower intensities, such as the one depicted in Figure 1 above. The task, therefore, is to identify and store only the main lobe in an embedded database designed for such signals.

One may note that the ideal case is symmetrical. Often this fact is relied upon to store only half the amount of data, considering that it is mirrored around the center frequency. In the case presented here, however, the non-symmetry of actual frequency data in the main lobe is important to the cybersecurity application under consideration and, thus, the entire main lobe is to be saved.

While many hardware and software solutions have been proposed for reducing side lobes in wireless signal DFTs, a simpler solution would be to trim the resulting DFT to include only the frequency bins of interest. This can also be referred to as cropping, although that term comes from image analysis with the data being removed being image data. Based on trimming as a proposed simplification applied to RF signals, the question then arises of whether or not it is feasible to identify the proper points at which the DFT should be trimmed.

The feature of a DFT being discrete is inherent in the need to trim data. The transform assumes that a selected window for the DFT calculation is the exact width of one or more full cycles of the waveform of interest. However, in reality, the window often cuts a particular waveform short of a full cycle (or whole number multiple of a full cycle). The result is an introduction of side lobes in the transform, representing frequency components that are artifacts of the math rather than frequencies that actually exist in the signals of interest. This is referred to as spectral leakage.

IV. SIGNAL PROCESSING

To identify the main lobe with the least computational effort, one might consider using the maximum intensity of a DFT as an indication of a location near its center. From there, the edges can be sought and the width calculated. The main lobe data must then be trimmed to be placed into a database, along with like entries from other signals received.

A. Step 1: Selecting the Main Lobe

To begin, a point is identified with a high probability of being located as a frequency bin within the main lobe. That would be a point with a high intensity. Thus, a function invoked to find the maximum value in an array of floating point numbers would be appropriate. If the DFT output is an array, using a maximum value function may remove the dimension of the array of interest, replacing it with a scalar value. Look for a function argument, like 'keepdims,' in cases where it is desired that the resulting dimension remain consistent with the original dimensions.

In practice, abnormalities exist in the DFTs measured in applications involving WiFi signals; abnormalities which will affect the selection of this point. These will be addressed in Section IV Laboratory Measurements, as well as in Section V Field Measurements. They will require altering this step. Until then, it is sufficient to say that the initial step is to identify a point of high intensity.

B. Step 2: Finding the Edges

Using a point with a high probability of residing in the main lobe as the starting point, it is now possible to examine lower, and then higher, frequency bins to find indications of the edges of the main lobe. In this portion of the process, low intensity is of more interest than high intensity. Finding the edges of the main lobe involves finding the points on either side of the point thought to be in the main lobe where the resulting value is first near zero; that is, near zero at the point closest to the maximum.

Actual measurements are never as clean as the ideal example, however. The main lobe, in fact, is often sprinkled with many points that are near zero. In fact, "zero" can mean some value close to the noise floor of the signal.

A moving-average acts as a low pass filter to smooth the normally jagged transform and provides a more stable value with which to compare some threshold value that is set near zero. A basic form of a moving average is the uniform moving average where the current frequency bin and the prior N-1 bins are summed and divided by N. This is equivalent to multiplying each frequency bin by 1/N and summing.

Yet, a moving average is not necessary. A moving summation accomplishes the same task without requiring a division operation each time a signal is received, nor does it require handling the special case where there could be an undesirable division by zero. Using a summation only requires adjusting the threshold by the number of samples in the moving summation.

In the proposed process, where generalization is desired, the threshold is set as a multiple of the center of the first quartile of sorted and ordered frequency bin intensities. For example, when collecting 12-bit data at 20M samples per second, one might receive a signal for which the DFT covers the full bandwidth of the receiver. However, it might also be far less than the full bandwidth. In either case, the center of the first quartile of sorted intensities most often carries some value close to the noise floor. By adjusting the multiplication factor of this value, a threshold may be chosen to appropriately mark the points at which the main lobe approaches zero (or really the noise floor).

This simple algorithm compares a moving summation incrementally moving away from the maximum, first in the lower frequencies, then in the higher frequencies. It increments until it reaches the limits of the data or falls below the threshold, at which point the bin in the summation window closest to the maximum is used to mark the low and high side of the main lobe; variable names *fftlo* and *ffthi*. The “fft” refers to the fundamental function, a Fast Fourier Transform [16].

C. Step 3: Matching the Database

To enter the selection into a database, one must consider the size allotted for each entry. If the simple difference, *ffthi-fftlo*, is either greater than or less than the entry size for the database, then the data must be manipulated to fit the database. In cases where the difference is less than the size allotted in the database, the DFT data is zero-padded on the side of the highest frequency bins.

It is important to note here that future comparisons of the padded data should take into consideration that the padding is not reflective of there being no high frequency components in the stored signal, but rather that the width of the main lobe is smaller than the allotted space. Thus, the values of the *fftlo* and *ffthi* should also be stored so the data retrieved may be viewed in proper context.

It is also important to note that padding the frequency domain data is not mathematically the same as padding the time domain data for a signal. In the case of the latter, resulting side lobes in a DFT can be accentuated as the window of data analyzed is artificially shortened.

On the other hand, the DFT of the received signal may be larger than that of the stored data. If the high-to-low difference is greater than the allotted space in the database, then the data must be trimmed again. In performing this operation, the center line between the *fftlo* variable and the *ffthi* variable is used to trim each the low and high ends of the available frequency bins such that the center remains the center of the trimmed data. This is done to preserve the most valuable portion of the data for later analysis or comparison. Thus, the allotted size is halved and points marked lower and higher by the length of each half are marked relative to the center line. This results in a main lobe that is of lesser width than the original.

V. LABORATORY MEASUREMENTS

Initially, a test was created to establish a baseline for future testing. In this case, the baseline would be defined as one with minimal multipath travel and a single, strong wireless signal to study.

A. Setup

An Ettus B210 Universal Software Radio Peripheral (USRP) is employed to receive two channels of synchronized data capture. This device features an Analog Devices two-channel 14-bit Analog-to-Digital Converter. Two RF Elements OARDSBX244 4 dBi Omni antennas are attached to the receive channels and placed in horizontal and vertical positions, with an angle of 90 degrees. A Netgear N600 wireless dual band router generates a periodic beacon broadcast on channel 10 (centered on 2.462GHz) to announce its presence to any listening devices.

In an outdoor setting with no measurable WiFi signals, the router is placed 10m from the antennas of the receiver. A recording is made of the electromagnetic signal with settings of 20M samples per second at a gain of 20.

The recording is used as input data to a pulse detection algorithm which extracts a single beacon in the form of a multidimensional array of complex numbers representing each sample pair for the horizontal and vertical inputs. That beacon is processed using Python’s library NumPy function *fft.fftn()* in an orthonormal mode, placing resulting vectors on a unit sphere. An FFT shift function is performed to place the frequency bins in order of lowest to highest along the x-axis.

B. Results

The resulting DFT, shown in Figure 2, produces an interesting result. The center point is not the maximum value. In fact, the main lobe dips in intensity at the center. This attribute is consistent over many tests. Thus, the algorithm was modified in Step 1 “Selecting the Main Lobe” to find the two highest points and take the center point between them to better reflect a point near the center of the main lobe. With the center point selected, the moving sums increment first forward and then backward from it to find the points at which the intensity is below the selected threshold.

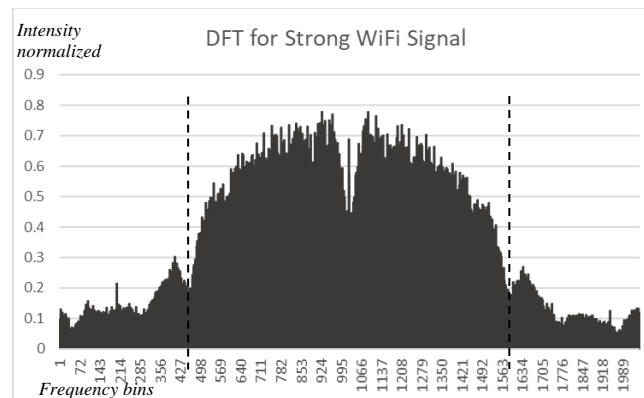


Fig. 2. A Unitized DFT for an example WiFi signal shown across frequency bins centered on 2.462GHz marking main lobe

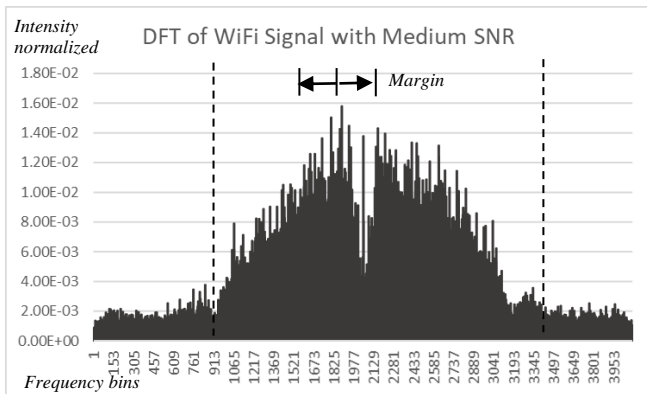


Fig. 3. A signal with lower SNR has a dip in the center approaching zero

The results of the selection process are shown in the same figure as dashed vertical lines demarking the low side and high side of the main lobe.

Moving the router farther away reduces the signal to noise ratio. The impact lessens the prominence of the main lobe making it slightly harder to identify. Nonetheless, the modification of using the two highest points continues to work. This is not obvious since the two highest points are now both to the left of center. But, since we are trying to identify a point with high probability of being in the main lobe, this point will suffice. One near the center would be more certain, but in this case, we are still well within the main lobe. The iteration to the higher frequencies will simply take longer than the iteration to the lower frequencies.

Now, however, it may be seen that the dip in the center is approaching zero. This could cause the method to select the center as one of the edges of the main lobe.

To compensate, the moving summations above and below the selected point begin on either side of a fixed margin around the center, in which we do nothing. Now, when incrementing to higher frequencies, the iterations will begin, not at the selected point, but at a fixed margin away from it, spanning the low center of the DFT.

This is the second modification made to Step 1. Figure 3 displays a signal with lower SNR and the resulting low and high points selected. Note in this image that a side lobe on the high frequency side of the main lobe was included in the selection erroneously. A minor adjustment lowering the multiplication factor on the threshold would resolve this.

VI. FIELD MEASUREMENTS

A. Setup

A site was selected with an indoor space approximating an industrial setting. A barn home was used with cross beams, fixtures in the space and miscellaneous objects which would produce a rich multipath channel for the RF signals to traverse. A barn home is one that is shaped like a barn, featuring a very large living space that has a 12x18 meter floor space and 12 meters ceiling. A USRP was placed along one wall of the facility.

The same router was placed at a point 9 meters in front of the receiving antennas and four Raspberry Pi 3B microcontrollers were placed on an arc 12 meters away from the receiving antennas and on positions relative to the plain of the two orthogonal antennas at angles of 60, 80, 100 and 120 degrees. The Pi's were programmed to connect with the router. Data was captured using the same parameters as the laboratory measurements.

All electrical devices in the house were shut down and interference studies were conducted with electrical fans and a microwave. The tests which follow were shown to have no electrical interference and no stray transmitters.

B. Results

In this environment, the SNR of some of the signals was much lower than those of the previous tests. The shape of the DFTs were also found to vary. The relative signal strength of received signals was not always as strong as those in the laboratory measurements. Their shape may be even less predictable than the lowest laboratory measurements, as may be seen in Figure 4, depicting the DFT for a WiFi signal with low SNR. It is much more difficult to see the main lobe, which extends over what seem to be two lobes rather than one.

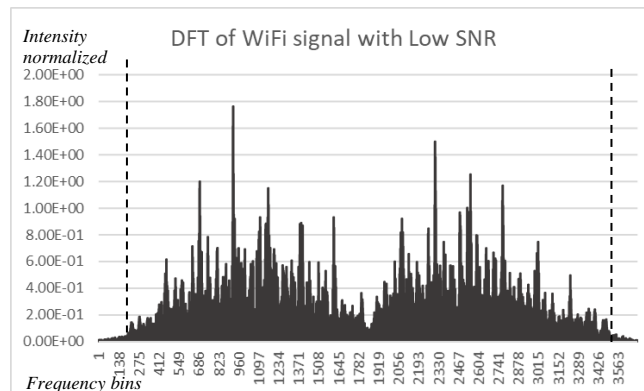


Fig. 4. DFT with low SNR causes the main lobe to be harder to determine

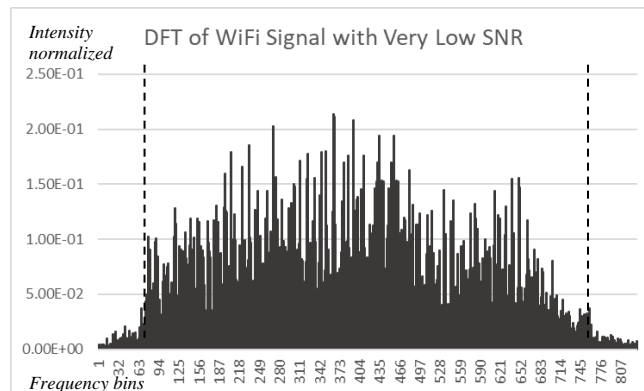


Fig. 5. When the SNR is low the dip in the center can be missing

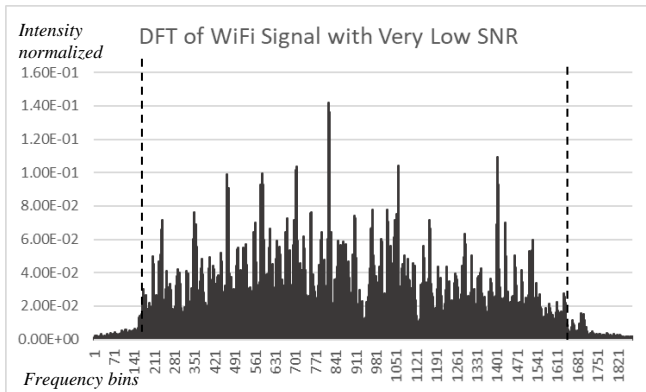


Fig. 6. Even lower SNR lessens the definition of the main lobe

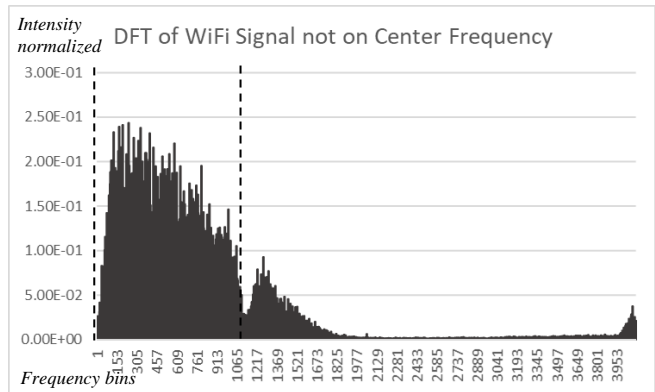


Fig.9. A DFT showing a WiFi signal captured from an adjacent channel

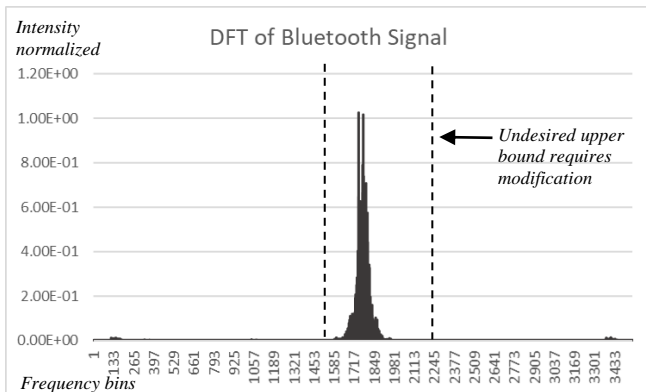


Fig. 7. A DFT of a Bluetooth signal is narrow with sidelobes farther away from the main lobe (before correction)

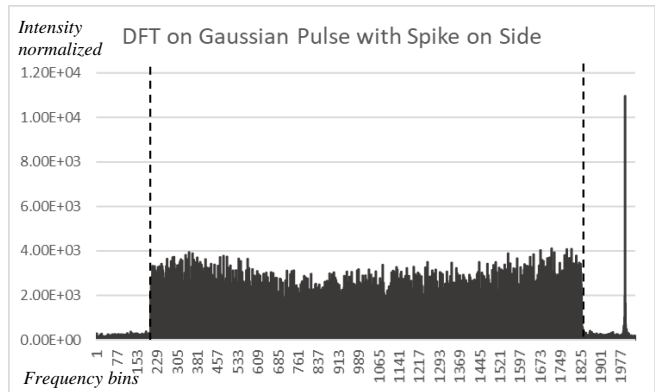


Fig. 10. DFT of a Gaussian pulse has a high intensity artifact that must not be counted as a peak intensity

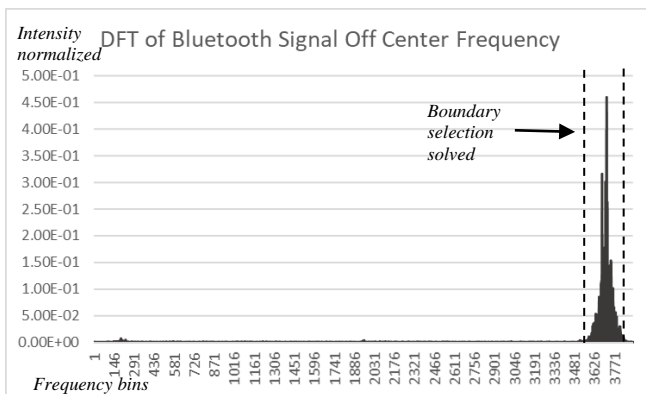


Fig. 8. A DFT of a Bluetooth signal centered on a different channel

On occasion, the dip seen in the previous tests was not present, as may be seen in Figures 5 and 6. Nevertheless, the algorithm for identifying the main lobe worked as modified.

A Bluetooth signal from one of the Pi's was recorded and analyzed. This signal is much more narrow than the previous WiFi signals and thus, the modification to have a fixed margin around the center that is not part of the calculations, along with the width of the window for a moving sum, each failed to accurately mark the low and high sides of this main lobe, as may be seen in Figure 7.

Bluetooth signals use a channel-hopping protocol and, thus, may appear in several locations across a fixed 20MHz receiver bandwidth. Figure 8 is an example of one that is not centered on the same channel.

In the particular cybersecurity application under consideration for use with this proposed process, the inclusion of data near zero causes problems in later analysis and, thus, is undesirable. As a result, narrow signals, like that depicted in Figures 7 and 8, are made exempt from these two interfering constraints. That is, the fixed margin to begin the sliding summation is not enforced and the window for the moving summation itself is removed, as seen in Figure 8. This is the third modification to Step 1 "Selecting the Main Lobe." The binary parameter marking a narrow band signal is stored along with the $fftlo$ and $ffthi$ parameters.

It should be noted that some signals may not be centered on the appropriate channel frequency, but may still be desirable to process. Such is a case depicted in Figure 9. Here, the signal is centered near the limit of the bandwidth of the receiver, which is approximately 20 MHz. The algorithm continues to perform appropriately in such cases with one boundary being selected as either zero or the maximum number of frequency bins, depending on which side of the desired channel it falls.

Lastly, the DFTs of some WiFi signals were seen to contain one point away from the main lobe with a very high

intensity. This typically occurred near an extreme of the receiver's bandwidth, likely from a dominant frequency in the noise floor, or as an artifact of the transform calculations. In either event, the errant point should not be used in the selection of the main lobe, as it is not in the main lobe. Figure 10 is an example of a case where there is a single point with a very high intensity. This is not a signal, per se, but rather a pulse of Gaussian energy like one may see emitting from a radar.

The fourth and final modification to Step 1, as a result, is to not use the first and second highest peaks, but instead use the second and third highest peaks to find a point with high certainty of being a part of the main lobe. Figure 8 depicts such a case, where the second and third peaks were used to find the boundaries of the main lobe efficiently.

With these four modifications made, approximately three thousand signals were studied and marked with selection of the main lobe for storage and retrieval from an embedded database. Only three were improperly marked and all three were signals with SNR less than 3 dB. The markings on all three truncated the main lobe on one side of the center point.

VII. CONCLUSION

Real time devices requiring use of an embedded database in RF signal applications must be efficient in terms of computing time. In cases where the frequency content is of particular interest, efficiency may be gained by carefully selecting only the main lobe resulting from discrete Fourier transforms and eliminating the side lobes and extraneous data on high and low sides.

Selecting the main lobe, however, can be hindered by several common abnormalities seen in the transforms of wireless signals; abnormalities like a dip in the center of the main lobe, the dip nearing the noise floor, and a single frequency outside the lobe with a very high intensity. In addition, some signals may be narrow band, requiring alternate handling.

Methods presented in this paper have been tested with a large number of varying cases and have shown to produce good results in selecting the proper main lobe information to offer efficient data storage and retrieval for further computation.

ACKNOWLEDGMENTS

The author extends his thanks to Dr. Thomas G. Pratt of the University of Notre Dame for his encouragement and experience in the use of the experimental settings and measurement equipment and also to Jay Labhart, Chief Technology Officer for Endpoint Security, for his knowledge of field conditions and assistance in the actual tests.

REFERENCES

- [1] T. G. Pratt and R. D. Kossler, "Input-to-Output Instantaneous Polarization Characterization," *IEEE Transactions on Antennas and Propagation*, Vol. 67, No. 3, pp. 1804-1818, March 2019.
- [2] R. P. Heller, T. G. Pratt, J. Loof and E. Jesse, "RF Biometric for Wireless Devices," In: Arai K., Bhatia R., Kapoor S. (eds)

- Proceedings of the Future Technologies Conference (FTC) 2018. FTC 2018. *Advances in Intelligent Systems and Computing*, vol 881. Springer Nature Switzerland AG, Cham. https://doi.org/10.1007/978-3-030-02683-7_65, October 2018.
- [3] J. Loof and T. G. Pratt, "Frequency-Hopped Signal Source Identification in Frequency-Selective Channels," *IEEE Transactions on Aerospace and Electronic Systems*, Vol. 55, Issue 6, pp. 3316-3329, December 2019.
- [4] J. Loof and T. G. Pratt, "Unsupervised Classification of Frequency-Hopped Signals in Frequency-Selective Channels," *Resilience Week, Denver Colorado, Best Cybersecurity Technology Paper Award*, pp. 108-113, *IEEE Cat. No. CFP18B24-POD*, ISBN 978-1-5386-6914-3, August 2018.
- [5] R. B. Blackman, "Linear Data-Smoothing and Prediction in Theory and Practice," January 1, 1965, Addison Wesley, 1st Edition, ISBN-10: 0201006103.
- [6] F. J. Harris, "On the use of Windows for Harmonic Analysis with the Discrete Fourier Transform," *Proceedings of the IEEE* 66(1): 51-83 doi/10.1109/PROC.1978.10837, January 1978.
- [7] J. Carnes, "Windowing High-Resolution ADC Data-PartI," *EETimes, Designlines*, February 4, 2009
- [8] S. V. Moholkar, "BER Performance for FFT and Wavelet Based OFDM Systems over AWGN Channel," *International Journal of Research and Scientific Innovation*, Vol II, Issue VIII, pp. 52-54, ISSN 2321-2705, August 2015.
- [9] A. N. Akansu and X. Lin, "A comparative performance evaluation of DMT (OFDM) and DWMT (DSBMT) based DSL communications systems for single and multitone interference," *Proceedings of the 1998 IEEE International Conference on Acoustics, Speech and Signal Processing, ICASSP '98* (Cat. No.98CH36181), Seattle, WA, USA, pp. 3269-3272 vol.6, doi: 10.1109/ICASSP.1998.679562, 1998.
- [10] I. Cosovic, S. Brandes and M. Schnell, "Subcarrier Weighting-A Method for Sidelobe Suppression in OFDM Systems," *IEEE Communications Letters* 10(6); pp. 444-446, DOI: 10.1109/LCOMM.2006.1638610, June 2006.
- [11] A. Selim and L. Doyle, "Real-time sidelobe suppression for OFDM systems using advanced subcarrier weighting," *IEEE Wireless Communications and Networking Conference*, pp. 4043-47. 10.1109/WCNC.2013.6555224, 2013.
- [12] A. Ilovitsh, T. Ilovitsh and K.W. Ferrara, "Multiplexed Ultrasound Beam Summation for Side Lobe Reduction," *Nature, Scientific Reports* 9, article 13961, <https://doi.org/10.1038/s41598-019-50317-7>, September 27 2019.
- [13] K. Sankhe et al., "ORACLE: Optimized Radio Classification through Convolutional neural Networks," in *IEEE INFOCOM 2019-IEEE Conference on Computer Communications*. IEEE, pp. 370-378, 2019.
- [14] S. Riyaz, K. Sankhe, S. Ioannidis, and K. Chowdhury, "Deep Learning Convolutional Neural Networks for Radio Identification," *IEEE Communications Magazine*, vol. 56, no. 9, pp. 146-152, Sept 2018.
- [15] A. Al-Shawabka et al., "Exposing the Fingerprint: Dissecting the Impact of the Wireless Channel on Radio Fingerprinting," *IEEE INFOCOM 2020 - IEEE Conference on Computer Communications*, Toronto, ON, Canada, pp. 646-655, doi: 10.1109/INFOCOM41043.2020.9155259, 2020.
- [16] M. T. Heidman, D. H. Burrus and C. S. Sidney, "Gauss and the History of the Fast Fourier Transform," *IEEE ASSP Magazine*, Vol 1, Issue 4, pp. 14-21, October 1984.